Impurity pinning of sliding charge-density waves

J. R. Tucker
Department of Electrical and Computer Engineering, University of Illinois, Urbana, Illinois 61801
(Received 6 March 1989)

A complete theoretical model is constructed to characterize the pinning of charge-density waves (CDW's) to individual impurity sites. The model is based upon consistently incorporating the microscopic CDW-impurity interaction calculated by Tüttó and Zawadowski within the large-scale Ginzburg-Landau framework of Lee and Rice. This analysis shows that the *local* CDW pinning by impurities will always be strong for all realistic values of the scattering parameter. On the other hand, the large-scale *average* CDW phase away from the impurity sites will be weakly pinned over extended volumes containing a great many individual impurities, in nominally "pure" crystals. This interplay between "weak" and "strong" aspects of the impurity pinning is found to explain most features of the experimental phenomenology, including the remarkable behavior seen in the broadband $1/f$-type noise spectrum above the depinning threshold.

I. INTRODUCTION

Charge-density-wave (CDW) conduction in quasi-one-dimensional metals represents the only known example of collective electron transport by a moving quantum ground state, apart from superconductivity. Since Monceau *et al.*[1] first observed the non-Ohmic behavior of $NbSe_3$ in 1976, this new conduction mechanism has attracted a great deal of interest, both experimental and theoretical. The experimental phenomenology has proved to be especially complex,[2] and a satisfactory theoretical interpretation has been very difficult to find. Enormous controversy has, in fact, permeated this entire field for several years, surrounding such issues as whether the impurity pinning should be taken as "weak" or "strong," quantum or classical. It now appears that a clear resolution of many of these basic issues is possible by combining two previous bodies of theoretical work. The first is the large-scale Ginzburg-Landau picture of CDW pinning put forward many years ago by Fukuyama, Lee, and Rice,[3,4] The second is the more recent microscopic calculation of the local impurity-CDW interaction by Tüttó and Zawadowski.[5] What remains is to consistently incorporate this microscopic calculation within the three-dimensional Ginzburg-Landau framework. In carrying out this procedure, we shall make several rough approximations that are consistent with solving the physical problem to within factors of ~ 2 or so, but not with mathematical artistry.

The basic result which emerges from this analysis is that the impurity pinning can always be represented as "strong," in the sense that the *local* CDW phase at the impurity site will remain close to its optimal value under most conditions. When the phase displacement in the surrounding region becomes sufficiently large, however, the amplitude of the order parameter is reduced within the immediate neighborhood of the impurity, eventually resulting in an advancement of the local phase through the process of phase slip. This type of local strong pinning is expected for virtually any impurity located on the metal sites of the CDW conducting chains, whether it is isoelectronic or not. The phase gradients surrounding each impurity site are confined to a very tiny volume in three dimensions, however, according to Ginzburg-Landau theory. The large-scale *average* CDW phase away from the impurity sites is thus predicted to remain correlated over rather large volumes, containing in excess of ~ 100 individual impurities for the dilute concentrations typical of nominally "pure" materials. The low-frequency ac response measured in equilibrium is therefore expected to be similar to "weak" pinning, since each individual impurity site does not dictate the value of the large-scale average phase.

In a previous work[6] based on the Ginzburg-Landau picture, we have proposed a phenomenological model for CDW dynamics by starting from the *a priori* assumption of strong pinning and phase slip at the individual impurity sites. This model and its subsequent extentions[7–9] have succeeded in providing a logically coherent and semiquantitative interpretation for the vast majority of experimental behavior observed in sliding CDW systems. The primary goal of the present work is to illustrate the microscopic basis for this model.

One of the last experimental areas that has not thus far been interpreted in terms of our strong-pinning model is the broadband $1/f$-type noise spectrum that appears when the CDW is in the sliding state above threshold. A series of recent experiments by Bhattacharya and coworkers[10–13] has uncovered several unusual, and initially very surprising, features of both the broadband noise (BBN) and the associated narrow-band noise (NBN). These results place serious constraints upon any theoretical interpretation of CDW dynamics. Our strong-pinning model naturally accounts for all major features of the observed noise spectrum, and this area provides an excellent opportunity to illustrate the relationship between the "strong" local impurity pinning and the "weak" large-volume dynamics displayed by the system.

II. MICROSCOPIC IMPURITY-CDW INTERACTION

In an important recent paper, Tüttó and Zawadowski[5] have demonstrated that the local interaction between the CDW and an individual impurity cannot be adequately described within Ginzburg-Landau theory. Their microscopic calculation shows that Friedel oscillations, having the same wavelength as the CDW, compete with the CDW's charge modulation over an atomic distance scale $x_0 \sim 10$ Å at the impurity site. If the impurity potential is sufficiently strong, these Friedel oscillations dominate the charge modulation within this highly localized region, and the phase of the Friedel oscillations becomes locked to its optimum value at the impurity site as illustrated in Fig. 1. The CDW, on the other hand, dominates the charge modulation at distances $x \gg \xi_0$ far away from the impurity, where $\xi_0 = \hbar v_F/\Delta \sim 30$ Å represents the Ginzburg-Landau amplitude coherence length. The force acting between the impurity and the CDW is then determined by the energy of mismatch within the region $x_0 < x < \xi_0$, as indicated by the dotted line in Fig. 1.

For simplicity, Tüttó and Zawadowski include only electron backscattering within their one-dimensional calculation. The perturbing Hamiltonian for a single impurity located at the origin is thus represented in the form

$$H_{\text{imp}} = T[\psi_R^\dagger(0)\psi_L(0) + \psi_L^\dagger(0)\psi_R(0)] \ . \tag{2.1}$$

Here, R and L refer to right- and left-moving electron states, respectively. The CDW in the absence of impurities is described in terms of an effective Fröhlich Hamiltonian, with an equilibrium Peierls gap given by

$$\Delta \approx 2D \exp(-1/s\hat{g}) \ . \tag{2.2}$$

The electronic bandwidth cutoff is here represented by D, and $s = 2$ when both spin components are included. The dimensionless electron-phonon coupling is given by $\hat{g} = -g(2k_F)/2\pi v_F$ in the usual notation.

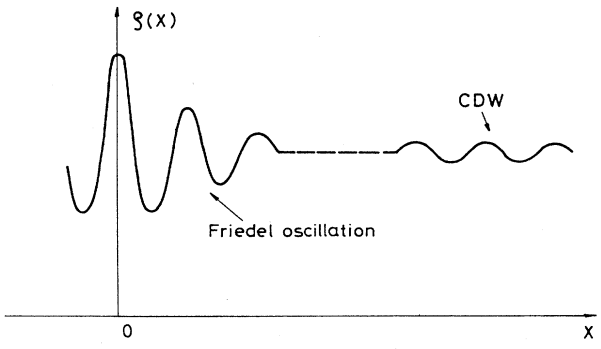

FIG. 1. Schematic plot of the electron density in the atomic neighborhood of an impurity site. The region of mismatch between the Friedel oscillations at the impurity location and the CDW's charge modulation at distances $x \gg x_0 \sim 10$ Å away from the impurity is indicated by the dashed line. Reproduced from Tüttó and Zawadowski (Ref. 5).

The numerical value of the electron-phonon coupling is $s\hat{g} \approx 0.2$ for all the inorganic sliding CDW materials. With this estimate, the impurity-CDW pinning force calculated by Tüttó and Zawadowski, and represented in Eqs. (6.9), (6.10), and Fig. 13 of their paper, may be approximately written in terms of an effective impurity potential in the form

$$V_{\text{imp}} \approx -\eta\Delta_0 \cos(\phi_0 - \phi_i) \ . \tag{2.3}$$

In this expression, the amplitude and phase of the CDW within the immediate neighborhood $|x| \ll \xi_0$ of the impurity site are represented by Δ_0 and ϕ_0, respectively, and ϕ_i is the optimal CDW phase, coincident with that of the Friedel oscillations. The strength of the impurity pinning is found to depend upon the dimensionless backscattering within this model according to

$$\eta = \begin{cases} 6.4(T/2\hbar v_F), & T/2\hbar v_F \ll 1 \\ 4, & T/2\hbar v_F \approx 1 \\ 2, & T/2\hbar v_F \gg 1 \ . \end{cases} \tag{2.4}$$

In the neighborhood of $T/2\hbar v_F \sim 1$, Tüttó and Zawadowski find that the effective potential becomes somewhat nonsinusoidal, as may be seen in their Fig. 13. We shall ignore this slight complication in the following discussion for the sake of simplicity.

In the weak-coupling limit, $T/2\hbar v_F \ll 1$, the CDW is only slightly distorted by the impurity, and the phase Φ of the charge modulation at the impurity site advances contiuosly along with the CDW's phase displacement ϕ_0, as illustrated in Fig. 2 for $T/2\hbar v_F = 0.04$ (after Tüttó and Zawadowski). For larger values of the backscattering, however, the charge modulation at the impurity site becomes fixed by the Friedel oscillations. Figure 2 shows that already for $T/2\hbar v_F = 0.08$, the phase of the charge modulation oscillates about its preferred value instead of following the CDW's displacement. Tüttó and Zawadowski estimate that the backscattering parameter

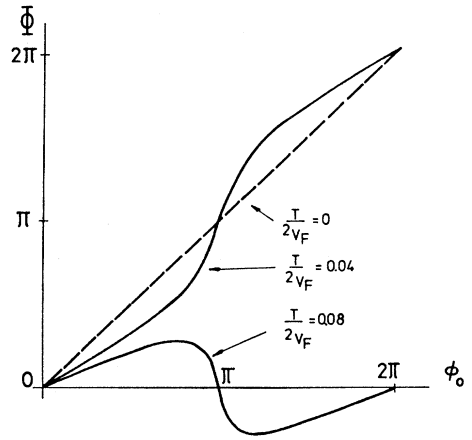

FIG. 2. Phase Φ of the charge modulation at the impurity site as a function of the local CDW phase ϕ_0, for different values of the dimensionless electron backscattering parameter. Reproduced from Tüttó and Zawadowski (Ref. 5).

will lie within the range $0.1 < T/2\hbar v_F < 1$ for typical impurities in sliding CDW systems, so that the Friedel oscillations are always expected to dominate the CDW charge modulation on an atomic scale near the impurity site.

An independent numerical estimate for the backscattering parameter can be made here by representing the impurity potential as a squarelike barrier of height V and width d, so that $T = Vd$ may be written in the form

$$\frac{T}{2\hbar v_F} \approx 0.8 \frac{V(\text{eV})d(\text{Å})}{v_F(10^7 \text{ cm s}^{-1})} . \tag{2.5}$$

The effective width of the barrier should be roughly comparable to the lattice constant, $a \approx 3.5$ Å for all the common sliding CDW materials. The Fermi velocity for $NbSe_3$ is universally estimated[14] as $v_F \approx 3 \times 10^7$ cm s^{-1}, and within a factor of ~ 2 or so of this value for the other sliding CDW materials. Use of these estimates in Eq. (2.5) yields $T/2\hbar v_F \approx 0.9 V(\text{eV})$, so that the dimensionless backscattering is approximately equal to the effective barrier height in electron volts.

In most sliding CDW systems, the electronic band structure can be well represented by a one-dimensional tight-binding band composed of d_{z^2} orbitals located on the transition-metal ions. For these materials, the effective impurity barrier may be simply estimated as the difference in atomic d-level energies, using Harrison's[15] Solid State Table, for example. The most common impurity in $NbSe_3$ is Ta, which is known to be present in ~ 100-ppm concentrations within the starting materials used in growing typical crystals.[16] For these two metals $\delta E_d = 0.46$ eV, so that our estimate for the backscattering based on Eq. (2.5) becomes $T/2\hbar v_F \approx 0.4$ in this case. Larger values are, of course, expected for nonisolectronic impurities such as Ti. Our estimates here are thus in good agreement with the range of backscattering parameters anticipated by Tüttó and Zawadowski. We also note that the present estimate $T/2\hbar v_F \approx 0.4$ for a Ta impurity on a Nb site (or a Nb impurity on a Ta site) is nearly an order of magnitude larger than the minimum value required in order for the Friedel oscillations to dominate the charge modulation at the impurity, according to Fig. 2.

III. INTEGRATION INTO THE GINZBURG-LANDAU FRAMEWORK

The microscopic impurity-CDW interaction calculated by Tüttó and Zawadowski describes only the local perturbation of the CDW in the immediate atomic neighborhood $|x| \ll \xi_0 \sim 30$ Å of the impurity site. The long-range deformations on a scale larger than ξ_0 must be calculated using Ginzburg-Landau theory, as originally outlined for three dimensions by Lee and Rice.[4] In their 1979 paper, Lee and Rice estimated the elastic energy of deformation that occurs when the CDW phase ϕ_0 near a single strong impurity site differs from the phase $\bar{\phi}$ established at infinity:

$$E_{\text{pin}} \approx \frac{\Delta}{4\pi^2}(\bar{\phi} - \phi_0)^2 . \tag{3.1}$$

The numerical coefficient appearing here has been obtained during the course of our previous work,[6] and is smaller by a factor of ~ 4 than in the Lee and Rice paper due to a more careful treatment of the crystal anisotropy. Phase gradients surrounding the single strong impurity site are found to be confined to the smallest possible volume in three dimensions: to a longitudinal distance $L_0 \approx 7\xi_0$ along the chain direction, and to the cross-sectional area A_0 of the individual chain containing the impurity.

When a dilute concentration of strong impurities is present, we previously demonstrated that the large-scale average phase $\bar{\phi}$ will remain correlated over extended volumes containing a large number of individual impurity sites, with small independent phase-gradient regions surrounding each impurity. The length of this phase-coherent region was estimated to be approximately given by the mean spacing, $L = 1/n_i A_0$, between consecutive impurities along the conducting chains. Since $L/a = 10^6/n_i(\text{ppm})$ and $a \approx 3.5$ Å, a typical value $L \approx 1$ μm corresponds to $n_i \approx 350$ ppm. In cross section, average phase coherence should extend over distances at least as large as the nearest-neighbor impurity spacing, $(L/a)^{1/3} A_0^{1/2}$, in the transverse directions. According to these estimates, the minimum number of impurities within a single phase-coherent region is approximately given by

$$N_i \approx (L/a)^{2/3} \approx 200[L(\mu\text{m})]^{2/3} . \tag{3.2}$$

Only at very high impurity concentrations $n_i > 10\,000$ ppm, where the small individual phase-gradient regions begin to overlap, will it become energetically favorable to smoothly interpolate the CDW's phase over the volume scale n_i^{-1} associated with a single impurity. This result was used as the starting point for our previous work on a phenomenological model for CDW dynamics, based on the assumption that the local impurity pinning may indeed be taken as strong and not weak. Prior to our work, the possibility that strong pinning could produce two qualitatively different overall phase configurations, depending upon impurity density, was very nicely described by in a paper by Abe[17] that has only recently come to our attention.

Returning now to the problem of a single isolated impurity, we can combine the result of Tüttó and Zawadowski for the impurity-CDW interaction , approximately given in Eq. (2.3), with the Ginzburg-Landau expression for the elastic energy of the local phase gradients, given in Eq. (3.1). In doing this, it is important to recognize that the CDW's amplitude Δ_0 at the impurity site will depend upon the magnitude of the surrounding phase gradients. If the impurity potential is sufficiently strong, large phase gradients can develop to the point where the CDW amplitude becomes depressed toward zero within a region $\sim \xi_0$ about the impurity site, initiating a phase-slip process. In the Appendix we have estimated that this depression of the CDW order parameter may be approximated in the form

$$\frac{\Delta_0}{\Delta} \approx \left[1 - \frac{(\bar{\phi} - \phi_0)^2}{\Theta^2} \right] , \tag{3.3}$$

where $\Theta \approx L_0/\xi_0 \approx 7$ according to Ginzburg-Landau theory. Combining Eqs. (2.3) and (3.1) then yields a total impurity pinning energy:

$$E_{\text{total}} \approx \tfrac{1}{2} k_{\text{elast}} (\bar{\phi}-\phi_0)^2 - k_{\text{imp}} \left[1 - \frac{(\bar{\phi}-\phi_0)^2}{\Theta^2} \right] \cos(\phi_0-\phi_i) \ . \tag{3.4}$$

The impact of amplitude suppression on the elastic energy in Eq. (3.1) is of order $[(\bar{\phi}-\phi_0)/\Theta]^4$, and is neglected here for simplicity. According to Eq. (3.1), the elastic constant associated with the phase-gradient region is approximately given by $k_{\text{elast}} \approx \Delta/2\pi^2$, and the strength of the CDW-impurity interaction, $k_{\text{imp}} = \eta\Delta$, may be estimated from the microscopic theory according to Eq. (2.4).

At zero temperature, the CDW phase ϕ_0 at the impurity site adjusts itself to minimize this total energy, yielding the condition

$$\left[1 - \frac{(\bar{\phi}-\phi_0)^2}{\Theta^2} \right] \sin(\phi_0-\phi_i) = \frac{2}{\Theta^2} (\bar{\phi}-\phi_0)[k' + \cos(\phi_0-\phi_i)] \ . \tag{3.5}$$

The behavior obtained within this model depends primarily upon the dimensionless ratio of elastic constants:

$$k' = \frac{\Theta^2 k_{\text{elast}}}{2k_{\text{imp}}} \ . \tag{3.6}$$

In the limit $k' \gg \Theta^2$ or $k_{\text{elast}} \gg k_{\text{imp}}$, the impurity potential is small compared to the phase-gradient energy and the pinning will be "weak." The CDW phase ϕ_0 at the impurity site closely follows the phase displacement $\bar{\phi}$ at large distances in this case, with only very small deviations $(\bar{\phi}-\phi_0) \approx (k_{\text{imp}}/k_{\text{elast}}) \sin(\phi_0-\phi_i)$ due to the impurity potential. When $k' \leq 1$, on the other hand, the local impurity interaction is sufficiently strong to cause phase slip at the impurity site as the CDW phase $\bar{\phi}$ at large distances is continuously advanced.

For simplicity in what follows we shall take $\Theta = 2\pi$, in rough agreement with the Ginzburg-Landau estimate quoted above. The expected range $0.1 < T/2\hbar v_F < 1$ of the backscattering parameter within the Tüttö and Zawadowski theory then implies a corresponding range for the dimensionless elastic constant given by

$$0.25 \leq k' \leq 1.5 \ . \tag{3.7}$$

Our numerical estimate of $T/2\hbar v_F \approx 0.4$ for a Ta impurity on a Nb site leads to the value $k' \approx 1$, and we shall adopt this as representative in our subsequent numerical work.

Let us begin by examining the predictions of this model for small displacements of the CDW phase away from its optimal value. Linearizing Eq. (3.5) yields

$$(\phi_0-\phi_i) \approx (\bar{\phi}-\phi_0) \left(\frac{2}{\Theta^2} + \frac{k_{\text{elast}}}{k_{\text{imp}}} \right) \approx 0.05(1+k')(\bar{\phi}-\phi_0) \ , \tag{3.8}$$

where $\Theta = 2\pi$ has been used in the final form. For $k' \approx 1$, the CDW phase ϕ_0 at the impurity site will be tightly pinned to its optimal value ϕ_i, with $(\phi_0-\phi_i) \approx 0.1(\bar{\phi}-\phi_0)$ according to these estimates. Deviations in the average phase $\bar{\phi}$ at large distances will thus produce very little displacement in ϕ_0 at the impurity site, with 90% of the total difference $(\bar{\phi}-\phi_i)$ contained within the phase gradients $(\bar{\phi}-\phi_0)$ surrounding the impurity site. We emphasize that in order to have "weak" pinning, the reverse would have to be true. That is, the CDW's phase ϕ_0 at the impurity site would need to remain close to the value $\bar{\phi}$ established at large distances, so that $\phi_0-\phi_i \gg \bar{\phi}-\phi_0$ for small displacements. According to Eq. (3.8), this would require a dimensionless elastic constant $k' > 100$. Unless our numerical estimates are in error by more than 2 orders of magnitude, therefore, the present model leads inescapably to the conclusion that the local impurity pinning will indeed be "strong" and not "weak."

The energy-minimization condition of Eq. (3.5) can be substantially simplified for $k' = 1$, the value estimated for a Ta impurity on a Nb site, to yield

$$\tan[(\phi_0-\phi_i)/2] = \frac{2}{\Theta^2} \frac{(\bar{\phi}-\phi_0)}{[1-(\bar{\phi}-\phi_0)^2/\Theta^2]} \ . \tag{3.9}$$

In this case, the total energy of Eq. (3.4) can also be rewritten in a simplified form:

$$E_{\text{total}} = 2k_{\text{imp}} \left[1 - \left[1 - \frac{(\bar{\phi}-\phi_0)^2}{\Theta^2} \right] \cos^2[(\phi_0-\phi_i)/2] \right] \ . \tag{3.10}$$

In Fig. 3 we have plotted the results of our numerical solution to Eq. (3.9), showing the local CDW phase displacement $(\phi_0-\phi_i)$ at the impurity site as a function of the total phase dispacement $(\bar{\phi}-\phi_i)$ at large distances.

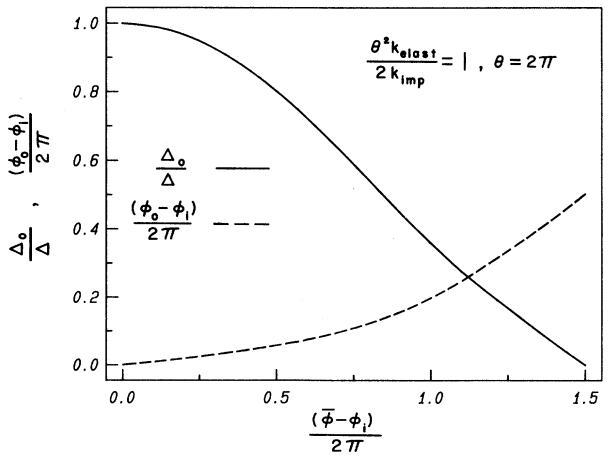

FIG. 3. Local CDW phase displacement $(\phi_0-\phi_i)/2\pi$ and amplitude Δ_0/Δ at the impurity site as functions of the total CDW phase displacement $(\bar{\phi}-\phi_i)/2\pi$ at large distances from the impurity, calculated according to Eqs. (3.9) and (3.3) with $k' = 1$ and $\Theta = 2\pi$.

Also included in Fig. 3 is our estimate for the CDW's amplitude Δ_0 near the impurity site, calculated according to Eq. (3.3). Figure 4 illustrates the resulting total pinning energy, as given by Eq. (3.10). The absolute energy scale here is $2k_{\rm imp}=\Theta^2 k_{\rm elast}\approx 2\Delta$ for $k'=1$ and $\Theta=2\pi$.

The physical picture which emerges from this calculation is relatively easy to interpret. As the CDW phase $\bar{\phi}$ at large distances becomes displaced from its optimum value ϕ_i, the local CDW phase ϕ_0 at the impurity site remains tightly pinned. For total phase displacements $(\bar{\phi}-\phi_i)/2\pi<0.6$, the local deviation is only $\phi_0-\phi_i\approx 0.1(\bar{\phi}-\phi_0)$, and this eventually produces large phase gradients in the region surrounding the impurity. When $(\bar{\phi}-\phi_i)/2\pi\approx 0.8$, the CDW's amplitude Δ_0 at the impurity site has been reduced to $\sim\frac{1}{2}$ of its equilibrium value Δ, and the maximum restoring force has been reached:

$$\left[\frac{\partial E_{\rm total}}{\partial\bar{\phi}}\right]_{\rm max}\approx -0.37\Delta\ . \tag{3.11}$$

This result is larger by a factor of ~ 4 than our previous crude estimate[6] for the maximum $T=0$ restoring force due to a single impurity. Further displacements in the CDW phase $\bar{\phi}$ at large distances will rapidly advance the local phase ϕ_0 and depress the CDW's amplitude Δ_0 at the impurity site, leading to total amplitude collapse at $(\bar{\phi}-\phi_i)/2\pi=1.5$ for this particular set of parameters ($k'=1$, $\Theta=2\pi$). If we assume purely relaxational dynamics, as in time-dependent Ginzburg-Landau theory, then the CDW order parameter will change sign as it passes through zero, so that the phase will instantaneously advance through π. This gives a local phase displacement $\phi_0-\phi_i=2\pi$, and the CDW's amplitude then regrows (almost instantaneously) in the optimum relative phase configuration.

A remnant polarization $(\bar{\phi}-\phi_0)/2\pi=0.5$ still remains, however, so that subsequent motion of the CDW in the same direction at $T=0$ produces a total effective pinning potential of the form sketched in Fig. 5. If the CDW motion is reversed by applying an electric field of opposite sign, then the initial current response will be enhanced by the discharge and reestablishment of this remnant polarization in the opposite direction. We propose this phenomenon as the source of the "overshoot" effects first observed by Gill,[18] and subsequently by many others. Recent liquid-helium–temperature experiments[19] on $K_{0.3}MoO_3$ have established that the magnitude of the remnant polarization corresponds to a displacement of the CDW through roughly $\frac{1}{2}$ wavelength, in agreement with the present model. All other observed features of the remnant polarization and "overshoot" phenomena also appear consistent with the picture outlined here.

IV. dc MOTION OF THE CDW CONDENSATE

The detailed interaction of the CDW with an individual impurity site has direct experimental consequences, in addition to the remnant polarization discussed in the preceding section. The most apparent of these is the characteristic temperature dependence of the depinning field. In all common sliding CDW materials, the average depinning field takes on the following functional form well below the Peierls transition:

$$E_0(T)=E_0(0)\exp(-T/T_0)\ . \tag{4.1}$$

The temperature scale is found to lie in the range $T_0\sim 10$–100 K, depending upon the material. In small crystals of high quality, the minimum threshold field E_T is approximately equal to E_0, and thus shows the same temperature dependence.[20] In less homogeneous samples the minimum threshold field E_T may assume a different dependence, but the average depinning field inferred from the complete dc I-V characteristic still follows the functional form given in Eq. (4.1).[21]

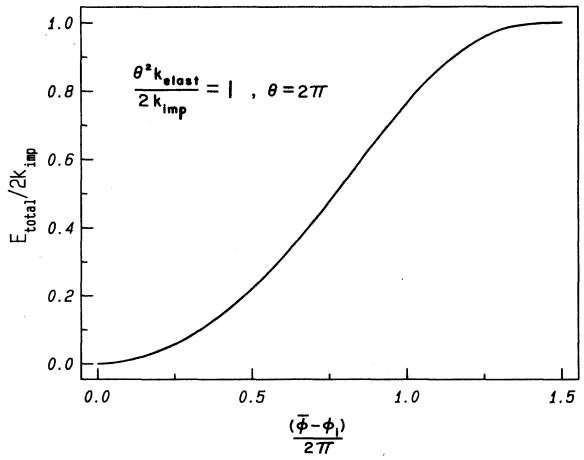

FIG. 4. Total CDW-impurity interaction energy under the conditions illustrated in Fig. 3, calculated from Eq. (3.10) with $k'=1$ and $\Theta=2\pi$.

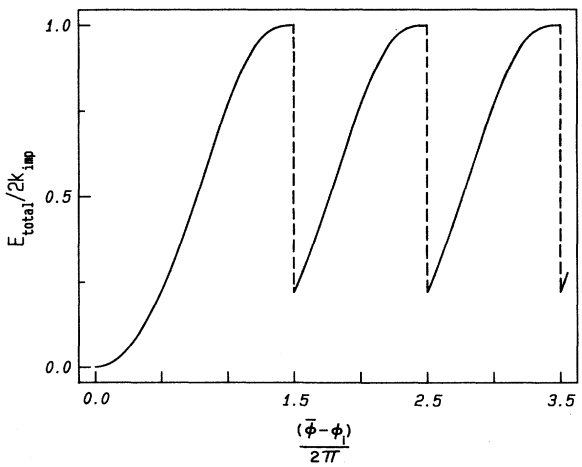

FIG. 5. Sketch of the total CDW-impurity interaction energy when the CDW's phase $\bar{\phi}$ at large distances is advanced continuously in the positive direction. A remnant polarization of π remains after each phase-slip event within this model for $k'=1$ and $\Theta=2\pi$.

In our previous theoretical work,[6] we explained this behavior in terms of independent thermal fluctuations occurring within the local phase-gradient regions surrounding each impurity site. The general nature of these fluctuations is illustrated in Fig. 6. When the impurity pinning is strong, as it will be in virtually all cases, the important thermal fluctuations are effectively confined to the neighborhood of these small phase-gradient regions. The energy scale for fluctuations in the large-scale average phase $\bar{\phi}$ will be greater by 1–2 orders of magnitude.

The equilibrium energy of the localized phase gradients is estimated in Eq. (3.1). Crudely speaking, we can approximate the important thermal fluctuations as local changes in the value of $\bar{\phi}-\phi_0$ near each site. For a sinusoidal pinning potential $V(\phi)=-V_{\max}\cos\phi$, the impact of such fluctuations may be easily taken into account according to a calculation given by Maki.[22] Convolving the sinusoidal form for the pinning energy with a Gaussian distribution of width $\langle\phi^2\rangle=k_BT/V_{\max}$ reduces the maximum pinning potential by a factor of $\exp(-T/T_0)$, where $T_0=2V_{\max}/k_B$. Although the actual pinning potential is nonsinusoidal, we can approximate $V_{\max}\approx\Delta/2\pi^2$ for small displacements to yield

$$T_0\approx\Delta/10k_B \ . \tag{4.2}$$

This rough estimate has been shown to be in good numerical agreement with experimental values for a variety of materials.

The total pinning potential for a large phase-coherent region will be approximately $(N_i)^{1/2}$ times that for an individual site, where N_i represents the total number of impurities contained within this region. The factor $\exp(-T/T_0)$ due to thermal fluctuations multiplies each term within the random sum, and thus appears directly in the overall pinning force. The fact that such a small temperature scale controls the depinning over a large phase-coherent region is a remarkable experimental finding, which is easily explained within the context of our strong-pinning model.

When the CDW becomes depinned above the threshold field E_T, the resulting dc motion at velocity v_d is accompanied by current oscillations or "narrow-band noise" at the average drift frequency $\omega_d=2k_Fv_d$ and its harmonics. We have previously shown[6] that the basic features of the NBN can be reproduced by using a simple relaxation-oscillator model, as illustrated in Fig. 7, to represent the CDW polarization and depinning within a single phase-coherent region. This relaxation-oscillator approach to interpreting the NBN was originally proposed on empirical grounds several years ago by Weger, Grüner, and Clark.[23] By reinterpreting it within the context of our strong-pinning model, we can relate the CDW's drift frequency ω_d in a dc field to the dielectric relaxation frequency ω_0 measured in ac-conductivity experiments:

$$\omega_d\approx\omega_0\left[\frac{E}{E_T}-1\right]\exp(-E_0/E) \ . \tag{4.3}$$

Here, ω_0 is identified with the $1/RC$ time scale of the relaxation-oscillator model, and E_T is proportional to the breakdown voltage. An additional factor $\exp(-E_0/E)$ has been included to account for the field dependence of CDW acceleration within a large phase-coherent region.[6] This expression has been shown to yield accurate numerical estimates for the CDW drift frequency in a variety of materials. At low temperatures, normal-carrier screening currents that are required in order to compensate for CDW polarization charges come to dominate the dissipation involved in CDW motion. In this regime, the dielectric relaxation frequency takes on an Arrehenius temperature dependence due to the scarcity of uncondensed electrons:

$$\omega_0\approx\frac{\sigma_N(T)}{\epsilon(\omega\rightarrow0)} \ , \tag{4.4}$$

Here, $\sigma_N(T)\sim\exp(-\Delta/k_BT)$ represents the normal-carrier conductance, and $\epsilon(\omega\rightarrow0)$ is the static dielectric constant.

A wide range of experiments has been quantitatively interpreted in terms of this simple relaxation-oscillator picture of the dc dynamics. The CDW drift frequencies observed at low temperatures are found to be accurately represented by Eqs. (4.3) and (4.4), displaying the Arrhenius temperature dependence of the dielectric relaxation frequency for constant values of E/E_T.[7] For relatively large electric fields $E>4E_T$ and drift frequencies

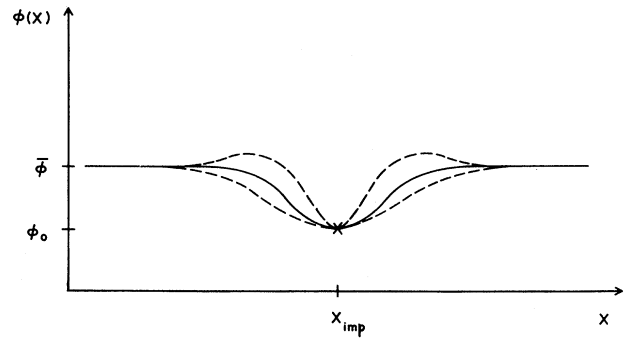

FIG. 6. Sketch of local thermal fluctuations in the CDW's phase configuration near a strong-pinning site.

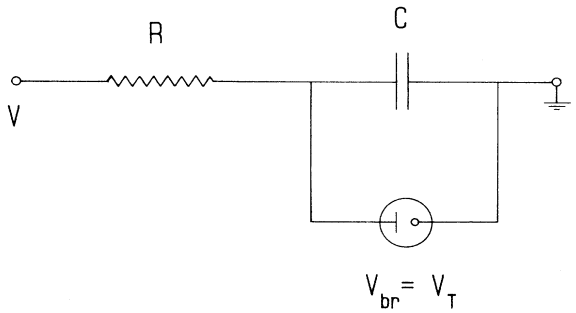

FIG. 7. Relaxation-oscillator model for CDW polarization and depinning within a single phase-coherent region, after Weger, Grüner, and Clark (Ref. 23).

$\omega_d > \omega_0$, the NBN amplitude and harmonic content become field independent, indicating a slightly nonsinusoidal but approximately constant effective pinning potential.[24] At low drift frequencies $\omega_d \ll \omega_0$, however, the harmonic content of the NBN is dramatically enhanced, reflecting the "jerky" motion expected in a relaxation oscillator just above threshold.

This "jerky" CDW motion for $\omega_d \ll \omega_0$ causes a dramatic postponement in the motional narrowing of the ^{93}Nb NMR linewidth in $NbSe_3$, as observed by Ross, Wang, and Slichter.[25] $NbSe_3$ is the only common sliding CDW material whose Fermi surface remains incompletely gapped by the Peierls transition, so that there is always an abundance of normal carriers and the dielectric relaxation frequency $\omega_0/2\pi \approx 10$ MHz remains relatively large and temperature independent. Motional narrowing of the NMR line in $NbSe_3$ is observed to occur not at an average dc drift frequency comparable to the static NMR linewidth $\Delta\omega/2\pi \approx 30$ kHz, but at a much larger value $\omega_d/2\pi \approx 15$ MHz near the dielectric relaxation frequency, and thus a factor of ~ 500 greater than would be expected for smooth CDW motion. In his Ph.D. thesis, Ross[26] attributed this striking effect to local motion of the CDW in rapid "jumps" of precisely 2π in phase separated by long stationary intervals, over the region $E < 4E_T$ near threshold. Several additional experiments were carried out to confirm that the CDW motion was relatively uniform throughout the multicrystal $NbSe_3$ sample used by Ross, Wang, and Slichter. The drift frequency $\omega_d/2\pi \approx 15$ MHz for onset of motional narrowing was also measured as the peak in the NBN fundamental, relacing the (lower) calculated estimate contained in the published paper. The locally "jerky" CDW motion inferred by Ross from his $NbSe_3$ NMR experiments is precisely that expected[7] within the context of the relaxation-oscillator model. There the current flows in sharp, widely spaced pulses of width $RC \approx 1/\omega_0$ at voltages near threshold, so that the CDW's motion should only become continuous for average drift frequencies $\omega_d > \omega_0$.

NMR experiments on $Rb_{0.3}MoO_3$ at low temperatures $40 < T < 60$ K, on the other hand, appeared to show qualitatively different results.[27] In this material, the completely gapped Fermi surface leads to a very small normal-carrier concentration within this temperature range, so that the dielectric relaxation frequency $\omega_0/2\pi \approx (3.2 \times 10^9\ \mathrm{s}^{-1})\exp(-829\ \mathrm{K}/T)$, as given by Eq. (4.4), becomes smaller than the static ^{87}Rb NMR linewidth $\Delta\omega/2\pi \approx 10$ kHz. Under these conditions, the motional narrowing is found to occur at a CDW drift frequency $\omega_d/2\pi \approx 5$ kHz comparable to the static linewidth. This behavior is also predicted by the relaxation-oscillator model, however, since in this case a dc drift frequency larger than the static linewidth already exceeds the dielectric relaxation frequency, so that the CDW motion should be relatively smooth in that regime. The controversy associated with these two apparently contradictory NMR results thus appears to be completely resolved: both are correct and easily understood within the context of the simple relaxation-oscillator model.

According to our interpretation, it should also be possible to observe "jerky" CDW motion in $Rb_{0.3}MoO_3$ as well, and this effect has recently been reported.[28] At dc current biases just above threshold, discrete voltage pulses are seen within separate regions of a small $Rb_{0.3}MoO_3$ crystal by employing multiple contacts. For higher electric fields, these pulses become the quasiperiodic current oscillations of the NBN. Near threshold, however, the individual voltage pulses are observed to propagate down the chain direction at a velocity of $\sim 0.3\ \mathrm{m\,s}^{-1}$ at a temperature of 77 K. This value for the propagation velocity can be readily understood in terms of the dielectric relaxation time $2\pi/\omega_0$ needed in order to readjust the CDW's configuration over a phase-coherence length L. Depinning of one region should result in a "domino effect," with the moving portion advancing at a speed approximately given by $L\omega_0/2\pi$. Our numerical estimate[7] quoted above for $Rb_{0.3}MoO_3$ gives a dielectric relaxation frequency $\omega_0/2\pi \approx 67$ kHz at $T = 77$ K. The relatively long phase-coherence length $L \approx 4\ \mu$m in blue bronze at low temperatures[9] thus implies a propagation velocity of $\sim 0.3\ \mathrm{m\ s}^{-1}$ at 77 K, in precise agreement with experiment. This propagation velocity is also found to follow an Arrhenius dependence as a function of temperature, with an activation temperature equal to that of the dielectric relaxation frequency within the accuracy of the measurements.

The dielectric relaxation frequency $\omega_0/2\pi \approx 67$ kHz at 77 K in $Rb_{0.3}MoO_3$ is much larger than the ^{87}Rb NMR linewidth $\Delta\omega/2\pi \approx 10$ kHz, in contrast to the situation at lower temperature $40 < T < 60$ K discussed above. Here motional narrowing of the NMR line should therefore be postponed by the locally "jerky" motion of the CDW near threshold, just as in $NbSe_3$. Indeed, the onset of motional narrowing at 77 K in $Rb_{0.3}MoO_3$ has been reported[29] near a drift frequency $\omega_d/2\pi \approx 70$ kHz, approximately equal to the dielectric relaxation frequency as expected according to our model.

The simple relaxation-oscillator model for local CDW motion within a phase-coherent region has thus allowed us to successfully interpret a very wide range of experimental phenomena associated with dc motion and the NBN. Recent work by Strogatz, Marcus, Westervelt, and Mirollo[30] indicates that many remaining aspects of the dc motion can be understood in terms of the collective behavior displayed by large numbers of such regions that are coupled together. While these collective effects are extremely interesting from the viewpoint of nonlinear dynamics, they reflect only indirectly on the microscopic interaction of the CDW with an individual impurity site. Fortunately, there is one additional feature of the dc CDW motion that displays the microscopic impurity pinning rather directly: the $1/f$-type "broadband noise" that is always observed as a low-frequency background to the NBN current oscillations.

V. ORIGIN OF THE BROADBAND NOISE

Broadband $1/f$-type noise is a generic phenomenon observed in a wide variety of electronic systems. The de-

pinning of a sliding CDW is observed to produce a very large BBN signal compared to systems involving only single-electron transport. While enormous compared to these more familiar sources of $1/f$-type noise, the BBN in CDW systems appears experimentally as a wide-spectrum background at frequencies near and below the discrete NBN peaks associated with the CDW "washboard" frequency. Although the BBN has been seen in CDW systems for many years, it is only through relatively recent experiments by Bhattacharya and coworkers[10–13] that the fascinating systematics of this phenomenon have been revealed. Here we shall briefly summarize the important experimental findings, and then offer our detailed interpretation.

In their initial study of the BBN, Bhattacharya *et al.*[10] reached the following conclusions: (1) the onset of the BBN is coincident with the onset of CDW motion, (2) the root-mean-square BBN voltage $\delta V(\omega)$ displays an $\omega^{-\alpha}$ spectrum approximately independent of electric field except near threshold, with $\alpha \approx 0.7$ for typical o-TaS_3 crystals, (3) the BBN noise voltage $\delta V(\omega)$ scales as $(l/A)^{1/2}$, where l is the sample length and A the cross-sectional area, so that $\delta V^2/V_T^2$ scales as the inverse volume. This result implies that the BBN is generated throughout the bulk, and not at the surface or contacts. The most important result obtained in this study was a clear demonstration that the observed BBN can be related to field-independent fluctuations in the overall threshold voltage V_T. In experiments at constant total current I, any fluctuations in V_T will cause changes in the total resistance $R = V/I$ of the sample, so that this mechanism should produce a noise voltage given by

$$\langle \delta V^2(\omega) \rangle_I = I^2 \left[\frac{\partial R}{\partial V_T} \right]^2 \langle \delta V_T^2(\omega) \rangle \ . \tag{5.1}$$

Assuming that R is a function of $V - V_T$ only, $\partial R/\partial V_T$ can be replaced with $-\partial R/\partial V$ and numerically evaluated from the dc I-V characteristic. Detailed comparisons of the BBN voltage $\delta V(\omega)$, measured at low frequencies, with the quantity $I(\partial R/\partial V)$ showed that they are virtually identical functions of both temperature and electric field. Bhattacharya *et al.* thus concluded that the BBN must be caused by fluctuations in the threshold voltage that are approximately independent of the experimental conditions. In view of their bulk origin, these threshold fluctuations were written in the form

$$\langle \delta V_T^2(\omega) \rangle = \frac{V_T^2}{N} S(\omega, T) \ , \tag{5.2}$$

where $N = Al/\lambda^3$ represents the total number of phase-coherent regions of volume λ^3 contained within the sample. $S(\omega, T)$ is a spectral weight factor whose functional form may depend upon temperature.

A second paper by Bhattacharya *et al.*[11] studied the NBN in detail, and determined the frequency and amplitude probability distributions for typical NBN peaks in the presence and absence of mode locking to an externally applied ac signal. Their basic conclusion here was that the finite spectral width of the NBN results (in good crystals) from temporal fluctuations in the local CDW drift frequency, and not from static spatial variations as had previously been supposed. Moreover, the width of the NBN peaks and the amplitude of the BBN were observed to track each other closely under a variety of experimental conditions, and from one material to another. They noted that for a constant dc current $I = I_{\rm CDW} + V/R_N$ applied to the sample, the BBN amplitude may be written in the form

$$\langle \delta V^2(\omega) \rangle_I = R_N^2 \langle \delta I_{\rm CDW}^2(\omega) \rangle = \left[1 - \frac{R_N}{R_D} \right]^2 \langle \delta V_T^2(\omega) \rangle \ . \tag{5.3}$$

Here, R_N is the normal resistance due to uncondensed electrons, and $R_D = dV/dI$ represents the total dynamic resistance at the dc bias point. The first relation here is mathematically trivial, but it shows that the BBN results directly from temporal fluctuations in the CDW current. In other words, the BBN and the spectral width of the NBN are one and the same. The second form of the relation is obtained within their phenomenological pinning-force-fluctuation model. Changes in $I_{\rm CDW}$ are assumed to result from fluctuations in the threshold voltage V_T, and $I_{\rm CDW}$ is taken to be a function of $V - V_T$ only.

The main features of the experimental phenomenology were shown to be consistent with this interpretation. The $Q\ (=\omega_d/\Delta\omega_d)$ of the NBN peaks increases linearly along with the average CDW drift frequency ω_d, since the fluctuations in $I_{\rm CDW}$ are approximately constant as a function of electric field far above threshold according to Eq. (5.3). When the NBN is mode locked to an external ac signal, the BBN is observed to vanish along with the spectral width of the NBN peaks. According to Eq. (5.3), the BBN vanishes on a mode-locked step not because the source of the fluctuations goes away, but because fluctuations in V_T can no longer change the differential resistance R_D away from the normal resistance R_N so long as the CDW drift frequency remains locked to an external ac signal. In a subsequent and more detailed study of mode locking, Bhattacharya *et al.*[12] demonstrated that noise-induced intermittency occurs as a precursor to complete mode locking. Histograms of the most probable washboard frequency over long time intervals showed that the system tends to jump between competing subharmonic steps, so that mode locking involves a competition between the deterministic nonlinear dynamics and the stochastic $1/f$-type noise.

In their most recent study, Bhattacharya *et al.*[13] infer a remarkable connection between the BBN observed when the CDW is in the sliding state and the small-signal ac conductivity measured in the pinned state. The dc bias in these experiments is adjusted so that the NBN lies entirely outside the range of their spectrum analyzer ($\omega_d > 5$ MHz), and the measured BBN spectrum is thus essentially field indepenent. The following relationship of the BBN amplitude to the pinned-state ac response is then found to be approximately obeyed:

$$\delta V(\omega) \approx \delta V_T(\omega) \propto \frac{{\rm Im}\epsilon^*(\omega)}{\omega} = \frac{{\rm Re}\sigma(\omega)}{\omega^2} \ . \tag{5.4}$$

The dielectric response function appearing here is defined by $\epsilon(\omega)=\epsilon_0+\sigma(\omega)/i\omega$. In typical o-TaS_3 samples at 120 K, the ac conductivity follows a power law well below the dielectric relaxation frequency, with $\mathrm{Re}\sigma(\omega)\sim\omega^x$ and $x\approx 1.3$. The BBN spectrum in this same region is found to fall off as $\delta V(\omega)\sim\omega^{-\alpha}$, with $-\alpha\approx -0.7=x-2$ as predicted by the above relation. When the temperature is lowered below ~ 140 K in these experiments, a broad peak appears in $\omega\,\delta V(\omega)$ within the measured spectral range, as shown in Fig. 8. The position of this peak as a function of temperature tracks the Arrhenius behavior of the dielectric relaxation frequency ω_0, experimentally defined as the peak in $\mathrm{Im}\epsilon(\omega)$ and theoretically represented in Eq. (4.4). Above the broad peak near ω_0, the magnitude of $\omega\,\delta V(\omega)$ falls off with increasing frequency, following the behavior previously observed in $\mathrm{Im}\epsilon(\omega)$.

The result contained in Eq. (5.4) is very extraordinary. At first sight, it appears to be a simple fluctuation-dissipation relation, but in this case the BBN spectrum $\delta V(\omega)$ is measured in the sliding state, while $\epsilon(\omega)$ is measured in the pinned state. The clear implication is that the CDW fluctuations that occur in the sliding state must be very similar to those occurring in the pinned state. In other words, the BBN spectrum indicates that the CDW remains pinned *even while it is moving.*

Our contention here is that all of these features of the BBN and NBN, so carefully extracted by Bhattacharya and co-workers over the past few years, can be readily explained within the context of our strong-pinning model, and that no other explanation appears plausible. The general form of the above fluctuation-dissipation relation is very easy to understand from this point of view. According to the picture of impurity pinning described in Sec. III, the local CDW phase ϕ_0 will remain strongly pinned at each impurity site even while the large-scale average phase $\bar{\phi}$ is advancing, except for brief intervals just before phase slip takes place. The basic features of the overall CDW phase configuration will then be the same in either the sliding state or the pinned state, with essentially the same types of thermal fluctuations.

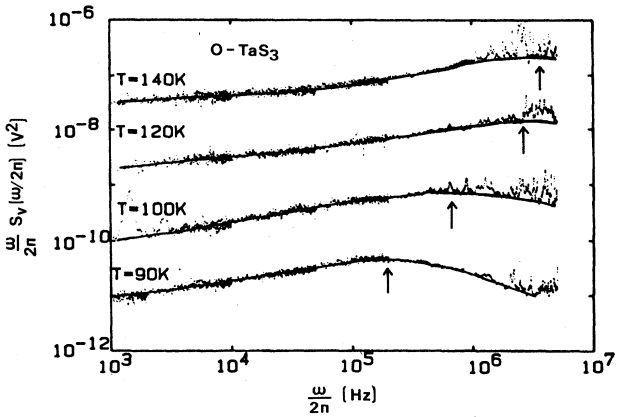

FIG. 8. Broadband-noise spectrum multiplied by frequency, $\omega S_V(\omega)$, for an o-TaS_3 crystal current biased far above threshold, so that the narrow-band noise lies beyond the frequency range of the measurements. The ordinate at each temperature is shifted for clarity. Solid lines are guides to the eye, and arrows mark the location of the most probable relaxation frequency. Reproduced from Bhattacharya *et al.* (Ref. 13).

To begin a detailed analysis, we now return to our discussion of the temperature dependence of the average depinning field, given in Eq. (4.1) of the preceding section. There it was estimated that thermal fluctuations in the localized phase gradients surrounding each impurity site are equivalent to a mean-square displacement $\langle\delta\phi^2\rangle \approx 2T/T_0$ in the potential of Eq. (3.1). This can be translated into a root-mean-square (rms) fluctuating force according to

$$\delta F_{\mathrm{rms}}\approx 2k_F\left.\frac{dE_{\mathrm{pin}}(\phi)}{d\phi}\right|_{\phi=\delta\phi_{\mathrm{rms}}} \approx 2k_F\frac{\Delta}{2\pi^2}\left[\frac{2T}{T_0}\right]^{1/2}\exp(-T/T_0)\ . \tag{5.5}$$

Adding random fluctuating forces from N_i individual impurity sites within a phase-coherent region then yields an estimate for the fluctuations in the total pinning force:

$$\delta F_T\approx(N_i)^{1/2}\delta F_{\mathrm{rms}}\ . \tag{5.6}$$

The total threshold force needed to depin a region containing N_i impurities is roughly that imposed by the average depinning field:

$$F_T\approx N_i(A_0L)\left[\frac{2k_F}{\pi A_0}\right]eE_0(T)\ . \tag{5.7}$$

Here, again, A_0 represents the cross-sectional area per CDW chain and L the average spacing between consecutive impurities. The volume per impurity is then $n_i^{-1}=A_0L$, and $n_c=2k_F/\pi A_0$ represents the CDW carrier density well below the Peierls transition.

Dividing the above two quantities, the relative fluctuations in the total pinning force for a single phase-coherent region may be written in the form

$$\frac{\delta F_T}{F_T}\approx\frac{1}{(N_i)^{1/2}}\frac{\Delta}{2\pi eE_0(0)L}\left[\frac{2T}{T_0}\right]^{1/2} \approx\left[\frac{T}{T_0}\right]^{1/2}\ . \tag{5.8}$$

In the final expression, we have utilized our previous estimate $E_0(0)\approx\Delta/4eL(N_i)^{1/2}$ for the $T=0$ depinning field, taken from Eq. (6.7) of Ref. 6. The result of Eq. (5.8) implies that within a single phase-coherent region the magnitude of the fluctuating force will roughly equal the net pinning force at $T\approx T_0$. Experimental crystals contain a very large number $N=Al/\lambda^3$ of phase-coherent regions, however, so that the fluctuations in the overall threshold voltage will be reduced by a factor of $1/\sqrt{N}$:

$$\frac{\delta V_T(\omega)}{V_T}\approx\frac{1}{\sqrt{N}}\left[\frac{T}{T_0}\right]^{1/2}f(\omega,T)\ . \tag{5.9}$$

Here we have included a spectral weight function $f(\omega,T)$ to indicate that the fluctuation spectrum must roll off

above some frequency that may depend upon temperature. Except for the additional factor of $(T/T_0)^{1/2}$, Eq. (5.9) is seen to be identical to the empirical relation given in Eq. (5.2). For the o-TaS_3 crystals used in the experiments of Bhattacharya *et al.*, the characteristic temperature is approximately $T_0 \approx 70$ K, so that the important temperature dependence should be contained within the spectral weight factor.

The form of the spectral weight function $f(\omega,T)$ is dictated by the fact that only low-frequency components of the local fluctuations occurring at the individual impurity sites will be effective in altering the value of the overall threshold voltage. Fluctuations in the total pinning force involve readjustments of the CDW's configuration over the volume of a phase-coherent region, and the time scale for this is limited by the dielectric relaxation frequency. If the dielectric response could be characterized by a single relaxation time ω_0^{-1}, then the spectral weight function would assume a simple Debye form:

$$f_0(\omega,T)=\frac{2}{\pi\omega_0}\frac{1}{[1+(\omega/\omega_0)^2]} . \tag{5.10}$$

The temperature enters here only through the Arrhenius behavior of the dielectric relaxation frequency ω_0 at sufficiently low temperatures. In real crystals, of course, there will be a broad distribution of relaxation times. In our previous work,[6] we derived a reasonably accurate representation for the low-frequency ac response by using a distribution function $P(\omega_p)=(\bar{\omega}_p/\omega_p^2)\exp(-\bar{\omega}_p/\omega_p)$ for the pinning frequency ω_p about its average value $\bar{\omega}_p=\pi c_0/L$, where c_0 is the unpinned CDW phason velocity. The form of this function is based upon a random distribution $P(l)=L^{-1}\exp(-l/L)$ in the phase-coherence length. Experimental results for $\sigma(\omega)$ were reproduced over a wide spectral region by convolving the distribution function $P(\omega_p)$ with the ac-conductivity expression for a single overdamped oscillator. While this procedure produced a correct overall shape for $\sigma(\omega)$, the very-low-frequency behavior $\mathrm{Re}\sigma(\omega)\sim\omega^{1.3}$, which reflects the $1/f$-type noise, cannot be modeled in such a simple way.

We can proceed empirically, however, by noting that the ac conductivity for the CDW, when represented as a single overdamped oscillator, may be written

$$\mathrm{Re}\sigma(\omega)=\frac{n_c e^2\tau}{M_F}\frac{\omega^2}{(\omega_{co}^2+\omega^2)} . \tag{5.11}$$

Here the "crossover frequency" is defined by $\omega_{co}=\omega_p^2\tau$, where τ represents the CDW damping parameter, and M_F is the inertial Fröhlich mass. For this single overdamped oscillator, the dielectric relaxation frequency ω_0, defined as the maximum in $\mathrm{Im}\epsilon(\omega)=-\mathrm{Re}\sigma(\omega)/\omega$, will be coincident with the "crossover frequency" ω_{co} that marks the rise in the ac conductivity. The static dielectric constant is approximately given by $\epsilon(\omega\to 0)\approx n_c e^2/M_F\omega_p^2$, so that the simple Debye relaxation spectrum of Eq. (5.10) may now be rewritten in the form

$$f_0(\omega,T)\approx\frac{\mathrm{Re}\sigma(\omega)}{\omega^2\epsilon(\omega\to 0)} . \tag{5.12}$$

When there is a broad distribution of relaxation times, as in real crystals, we should expect that this relationship will still be approximately satisfied, since in this case it represents a superposition in the linear ac response for a distribution of oscillator strengths. With $f(\omega,T)$ characterized in terms of the measured ac conductivity by this relation, our expression for the threshold fluctuations in Eq. (5.9) becomes

$$\delta V_T(\omega)\approx\frac{V_T}{\sqrt{N}}\left[\frac{T}{T_0}\right]^{1/2}\frac{\mathrm{Re}\sigma(\omega)}{\omega^2} . \tag{5.13}$$

Here, again, $N=Al/\lambda^3$ represents the total number of phase-coherent regions within the sample. This result is seen to be essentially identical to the experimental relations inferred by Bhattacharya *et al.*, and quoted in Eqs. (5.2) and (5.4). The entire experimental phenomenology associated with the BBN and NBN can thus be understood in terms of strong impurity pinning, by employing the approximate theoretical result of Eq. (5.13) within their phenomenological pinning-force–fluctuation model.

It is important to note how easily our strong-pinning theory accounts for all of the remarkable experimental behavior seen in the BBN and NBN. Thermal fluctuations in the localized phase gradients surrounding each impurity site produce random forces, which add incoherently within large phase-coherent regions to produce fluctuations in the overall threshold voltage. The spectrum of the localized fluctuations at the individual impurity sites is effectively "white," since the ac-conductivity resonance associated with this length scale is experimentally observed in the far infrared.[8] The spectral dependence of the threshold fluctuations is then determined by that of the dielectric response function, which sets the time scale for distorting the CDW's phase configuration over large volumes. Because the local phase remains pinned at each of the impurity sites even while the CDW is moving, fluctuations in the threshold voltage within the sliding state are approximately the same as they are in the pinned state, independent of electric field. These fluctuations may therefore be inferred from the equilibrium ac response through a fluctuation-dissipation relation.

It is also important to appreaciate that the experimental phenomenology discussed here can*not* be understood, even qualitatively, in terms of a weak-pinning model. With weak pinning, the CDW phase is not optimized at each impurity site, but distorts gradually over a large volume containing many impurities in order to reduce its net potential energy. The scale of these gradual phase distortions along the chain direction is given, in equilibrium, by the so-called "Lee-Rice length." This Lee-Rice length turns out to be inversely proportional to the impurity concentration, and within the notation of the present paper it may be written in the form

$$L_{LR}\approx\left[\frac{k_{elast}}{k_{imp}}\right]^2 L . \tag{5.14}$$

Here, $L=1/n_i A_0$ again represents the average impurity spacing along a single conducting chain. In Sec. II we saw that weak pinning requires $k_{elast}\gg k_{imp}$, so that

$L_{LR} \gg L$. When the CDW becomes depinned in an electric field, the maximum drift frequency ω_d at which it can quasistatically optimize its phase configuration over the length scale L_{LR} will be approximately limited to the dielectric relaxation frequency ω_0. At higher drift frequencies, the CDW is able to relax only over a shorter length scale, $L_{LR}(\omega_0/\omega_d)^{1/2}$, during one cycle of the dc motion. For very high electric fields and drift frequencies, therefore, the equilibrium phase distortions on the scale L_{LR} disappear, and only small-amplitude, short-wavelength disturbances near the impurity sites remain. In this regime the CDW phase will be nearly spatially uniform, negligibly perturbed by the weak impurity potentials. In view of these drastic changes in the characteristic CDW phase configuration over a wide range in electric field, it seems implausible that field-independent fluctuations in the overall threshold voltage could be obtained within this type of model. The experimental relationship between the threshold fluctuations in the moving state and the ac response measured in the pinned state, given in Eq. (5.4), thus appears to close the door on an interpretation of CDW dynamics based upon the assumption of weak pinning.

VI. CONCLUSIONS

In the first part of this paper, we have presented a detailed picture of the CDW's interaction with a single impurity. This has been achieved by consistently incorporating the microscopic impurity-CDW potential calculated by Tüttó and Zawadowski[5] within the large-scale Ginzburg-Landau framework of Lee and Rice.[4] The result indicates that the *local* CDW pinning will always be "strong," in the sense that the CDW's phase at the impurity site will remain close to the optimum value that matches the localized Friedel oscillations. When the CDW phase at large distances does not coincide with this optimum value, the impurity will be surrounded by a small region of rapid phase gradients, confined approximately to a distance $L_0 \approx 7\xi_0$ along the chain direction and to the cross-sectional area A_0 of a single conducting chain. For the impurity concentrations $n_i \ll 10\,000$ ppm of typical CDW crystals, these small phase-gradient regions will not overlap one another. The *average* CDW phase away from the impurity sites will then remain correlated over volumes much larger than the volume n_i^{-1} associated with a single impurity. Since this large-scale average phase is not dictated by the individual impurities, many qualitative features of the low-frequency response are predicted to be similar to those expected for "weak" pinning.

Aside from a more detailed picture of the impurity-CDW interaction, two new results emerge that were not anticipated in our previous work: (1) Numerical estimates indicate that for a typical isoelectronic impurity (a Ta atom on a Nb site) the strength of the interaction should be marginally sufficient to cause complete CDW amplitude collapse and phase slip at the impurity site during dc motion. Smaller electron backscattering would result in a large, but not complete, suppression of the CDW's amplitude at the impurity site prior to rapid advancements in the local phase. "Weak" pinning, on the other hand, would require an impurity-CDW interaction smaller by a factor of ~ 100 than our estimate, much too small for any type of metallic impurity located on the CDW conducting chains. (2) The process of phase slip (or substantial amplitude suppression) at a strong impurity site will incorporate a "remnant polarization" into the phase gradients surrounding each impurity for continuous dc motion in the same direction. When the direction of the electric field is reversed, the release of this remnant polarization will produce the types of "overshoot" phenomena[18] that have been experimentally observed for many years. Our estimates indicate that the magnitude of this remnant polarization corresponds to a CDW displacement of $\sim \frac{1}{2}$ wavelength, in agreement with recent low-temperature measurements.[19]

Because the small phase-gradient regions surrounding each impurity remain nonoverlapping for reasonable densities, independent thermal fluctuations of the CDW's phase configuration will occur at each site. The relatively small energy scale for these individual fluctuations then leads to the rapid thermal variation in the depinning field observed in CDW materials at low temperatures. In order to affect the overall pinning energy within a large phase-coherent region, however, the independent fluctuating forces originating near each impurity must couple through the dielectric response function, which limits the time scale for large-volume distortions of the CDW's phase configuration. The resulting spectrum of fluctuations in the total threshold voltage $\delta V_T(\omega)$ will thus roll off above the dielectric relaxation frequency. The dielectric relaxation frequency in fully gapped materials becomes temperature activated at low temperatures, $\omega_0 \approx \sigma_N(T)/\epsilon(\omega \to 0)$, and the peak in $\omega \delta V_T(\omega)$ is experimentally observed to track ω_0 as a function of temperature,[13] as expected according to our model. At constant temperature, the spectrum of $\delta V_T(\omega)$ has been shown to be approximately independent of electric field.[10] This is also to be expected, since the CDW remains strongly pinned at each impurity site during dc motion, except for brief intervals just prior to phase slip. The most compelling experimental result obtained by Bhattacharya *et al.*[13] is the fluctuation-dissipation relationship they have inferred between the BBN voltage fluctuations observed in the *sliding* state and the dielectric response function measured in the *pinned* state. This relation clearly implies that the essential features of impurity pinning do not, in fact, change in any important way as the CDW undergoes dc motion.

In our original work on a strong-pinning theory for CDW dynamics,[6] we used a series of simple models to characterize various aspects of the experimental phenomenology. We endeavored, however, to consistently link these various pieces together to form an overall picture of the CDW system, based upon our *a priori* assumption of strong impurity pinning within the Ginzburg-Landau framework. By making numerical estimates for the parameters in the model, we were able to quantitatively interpret a very broad range of experiments. Subsequent work[7-10] showed that additional experimental areas, involving qualitatively new phenomena, could also be suc-

cessfully interpreted within our strong-pinning theory. The present paper essentially completes this process. Here we have shown how the microscopic impurity-CDW interaction indeed produces the type of strong pinning and phase slip that was previously hypothesized. In addition, we have shown that the well-known "overshoot" effects have their origin in the remnant polarization of the microscopic impurity-CDW interaction (not in some unspecified set of "metastable states"), and that the many extraordinary properties seen in the broadband-noise spectrum may also be understood as a direct consequence of strong impurity pinning. Since these two topics were the only major experimental areas which had not been previously addressed, we consider that the broad outlines for a successful theory of pinning and dynamics in sliding CDW systems are now in place.

ACKNOWLEDGMENTS

During the course of this work, I have benefited from many discussions with W. G. Lyons, who collaborated extensively with me on the analysis of experimental data within the context of the phenomenological model of strong pinning that he and I have generated. S. Bhattacharya and I had numerous discussions related to his experiments on the BBN and NBN, and he has kindly provided some of his data prior to publication. I thank A. Zawadowski for a critical reading of the manuscript, and for many helpful comments. I am also indebted to P. B. Littlewood and John Bardeen, who motivated me to complete this theory of strong impurity pinning in sliding CDW systems. This work has been supported by the U.S. National Science Foundation (under Grant No. NSF-DMR-87-15431) and by the U.S. Joint Services Electronics Program (under Contract No. N00014-84-C-0149).

APPENDIX

Consider that the CDW's phase is fixed at ϕ_0 by interaction with an impurity located at $x=0$. When a different phase $\bar{\phi}$ is established at large distances from the impurity site, our previous three-dimensional Ginzburg-Landau estimate[6] shows that the resulting phase gradients will be confined within a distance $L_0 \approx 7\xi_0$ near the impurity site along the chain direction, and to the cross-sectional area A_0 of the individual chain containing the impurity. The gradient energy associated with these distortions is estimated in Eq. (3.1).

Sufficiently large phase gradients near a strong impurity will be capable of depressing the magnitude Δ_0 of the CDW order parameter within a distance $\sim\xi_0$ at the impurity site. We need to estimate this suppression, because the Tüttő-Zawadowski theory of the microscopic impurity-CDW interaction depends upon the value of Δ_0 over atomic distances at the impurity's location, through the results quoted in Eqs. (2.3) and (2.4). Ideally, one would like to solve the three-dimensional Ginzburg-Landau model for $\Delta(r)$ and $\phi(r)$ as functions of the total CDW phase displacement $(\bar{\phi}-\phi_i)$. The fact that the transverse amplitude coherence length $\xi_\perp \approx 1$ Å is smaller than the average interchain spacing $(A_0)^{1/2} \approx 7-8$ Å represents an added complication. In the absence of such a complete solution, however, we can still make a reasonable estimate for the amplitude suppression at the impurity site.

The Ginzburg-Landau expression for the free energy density in one-dimension and at $T=0$ may be written in the form

$$\frac{f(\psi)}{f_0} = -|\psi|^2 + \tfrac{1}{2}|\psi|^4 + \xi_0^2 \left| \frac{\partial \psi}{\partial x} \right|^2 = -|\psi|^2 + \tfrac{1}{2}|\psi|^4 + \xi_0^2 \left[\frac{\partial |\psi|}{\partial x} \right]^2 + \xi_0^2 |\psi|^2 \left[\frac{\partial \phi}{\partial x} \right]^2 . \tag{A1}$$

Here, $\psi = |\psi| e^{i\phi}$, and the order parameter has been normalized so that $|\psi|=1$ for a uniform system in equilibrium. The maximum condensation energy per unit volume is then $f_0/2 \approx \Delta^2/2\pi\hbar v_F$ per conducting chain. From our previous three-dimensional estimates, we know that outside the region of rapid phase gradients the magnitude and phase of the order parameter will be approximately constant, so that $|\psi|=1$ and $\phi=\bar{\phi}$ for $|x|>L_0$. Within a very small distance $\ll\xi_0$ of the impurity site, the CDW's amplitude and phase may also be taken as constants, $|\psi|=|\psi_0|$ and $\phi=\phi_0$, respectively. Averaging over the length $\sim 2L_0$ containing the phase gradients, we can therefore make the following rough approximations:

$$\langle |\psi|^2 \rangle \approx |\psi(x=L_0)|\,|\psi(x=0)| \approx |\psi_0| , \quad \left\langle \frac{\partial |\psi|}{\partial x} \right\rangle \approx \frac{1-|\psi_0|}{L_0} , \quad \left\langle \frac{\partial \phi}{\partial x} \right\rangle \approx \frac{\bar{\phi}-\phi_0}{L_0} . \tag{A2}$$

Inserting these approximations into the Ginzburg-Landau expression yields an average energy density:

$$\frac{f(|\psi_0|,\phi_0)}{f_0} \approx -|\psi_0| + \tfrac{1}{2}|\psi_0|^2 + \frac{(1-|\psi_0|)^2}{(L_0/\xi_0)^2} + |\psi_0| \frac{(\bar{\phi}-\phi_0)^2}{(L_0/\xi_0)^2} . \tag{A3}$$

Since $L_0 \approx 7\xi_0$, the third term may be neglected for simplicity. Minimizing the energy with respect to $|\psi_0|$ then gives

$$|\psi_0| = \frac{\Delta_0}{\Delta} \approx \left[1 - \frac{(\bar{\phi}-\phi_0)^2}{(L_0/\xi_0)^2} \right] . \tag{A4}$$

By this estimate, Δ_0 vanishes when the phase displacement reaches $\Theta \approx L_0/\xi_0 \approx 7$, which corresponds to roughly one wavelength. The estimated increase in free energy may be obtained by inserting the result of Eq. (A4) back into Eq. (A3):

$$\delta F \approx 2L_0[f(|\psi_0|,\phi_0)+f_0/2]$$
$$\approx \frac{2\Delta}{\pi^2}\frac{(\bar{\phi}-\phi_0)^2}{(L_0/\xi_0)}\left[1-\frac{1}{2}\frac{(\bar{\phi}-\phi_0)^2}{(L_0/\xi_0)^2}\right]. \quad \text{(A5)}$$

Note that for $L_0=8\xi_0$ the first term here is identical to the estimate given for the gradient energy in Eq. (3.1). The second term will be neglected, since it represents a relatively small correction prior to amplitude collapse that does not alter the essential behavior characterized in Sec. III. Other higher-order terms of this type have already been discarded by neglecting the third term in Eq. (A3).

A nearly identical result to Eq. (A4) for the amplitude suppression may be obtained by employing the model CDW Hamiltonian proposed by Inui *et al.*[31] The virtue of this model is that it provides a correct representation for the amplitude modes as well as the phase modes of the unpinned system, and also a simple form for their coupling. Inui *et al.* have utilized this model to characterize the dynamics of phase-slip processes occurring at widely spaced strong-pinning centers in one dimension. Their results presumably reflect the effects of dislocations and other extended defects across a large number of parallel neighboring chains in three dimensions. They show that the behavior of "switching" crystals, those which demonstrate an abrupt and hysteretic onset of CDW current at threshold, can be reproduced by the phase-slip phenomena calculated within this model. To analyze the problem of a single strong impurity embedded within three-dimensional crystal, we have artificially imposed the constraint that the phase gradients must be confined to a length $L_0\approx 7\xi_0$ about the impurity site in this one-dimensional model, just as we did in the one-dimensional version of Ginzburg-Landau theory given above. By making the same kinds of approximations given in Eq. (A2), the result we obtain for amplitude suppression at the impurity site within the model of Inui *et al.* becomes

$$\frac{\Delta_0}{\Delta}\approx\left[1-\frac{\pi^2\lambda}{4}\frac{(\bar{\phi}-\phi_0)^2}{(L_0/\xi_0)^2}\right]. \quad \text{(A6)}$$

Here, λ represents the dimensionless electron-phonon coupling constant $s\hat{g}\approx 0.2$, so that $\pi^2\lambda/4\approx\frac{1}{2}$ and the value of Θ is increased by $\sim\sqrt{2}$ relative to the Ginzburg-Landau result of Eq. (A4). This difference is insignificant, because it lies within the uncertainty of our approximations.

[1] P. Monceau, N. P. Ong, A. M. Portis, A. Meerchaut, and J. Rouxel, Phys. Rev. Lett. **42**, 1423 (1976).

[2] P. Monceau, in *Electronic Properties of Inorganic Quasi-One-Dimensional Compounds,* edited by P. Monceau (Reidel, Dordrecht, 1985), Pt. II, p. 139; G. Grüner and A. Zettl, Phys. Rep. **119**, 117 (1985).

[3] H. Fukuyama and P. A. Lee, Phys. Rev. B **17**, 535 (1978).

[4] P. A. Lee and T. M. Rice, Phys. Rev. B **19**, 3970 (1979).

[5] I. Tüttó and A. Zawadowski, Phys. Rev. B **32**, 2449 (1985).

[6] J. R. Tucker, W. G. Lyons, and G. Gammie, Phys. Rev. B **38**, 1148 (1988).

[7] J. R. Tucker, Phys. Rev. Lett. **60**, 1574 (1988).

[8] W. G. Lyons and J. R. Tucker, Phys. Rev. B **38**, 4303 (1988).

[9] J. R. Tucker and W. G. Lyons, Phys. Rev. B **38**, 7854 (1988).

[10] S. Bhattacharya, J. P. Stokes, M. O. Robbins, and R. A. Klemm, Phys. Rev. Lett. **54**, 2453 (1985).

[11] S. Bhattacharya, J. P. Stokes, M. J. Higgins, and R. A. Klemm, Phys. Rev. Lett. **59**, 1849 (1987).

[12] S. Bhattacharya, M. J. Higgins, J. P. Stokes, and R. A. Klemm, Phys. Rev. B **38**, 10 093 (1988).

[13] S. Bhattacharya, J. P. Stokes, M. J. Higgins, and M. O. Robbins, Phys. Rev. B (to be published).

[14] See for example, J. R. Tucker *et al.*, Ref. 6, p. 1154; G. Grüner and A. Zettl, in the second of Ref. 2, p. 139.

[15] W. A. Harrison, *Electronic Structure and the Properties of Solids* (Freeman, San Francisco, 1980).

[16] J. W. Brill, N. P. Ong, J. C. Eckert, J. W. Savage, S. K. Khanna, and R. B. Somoano, Phys. B **23**, 1517 (1981).

[17] S. Abe, J. Phys. Soc. Jpn. **55**, 1987 (1986).

[18] J. C. Gill, Solid State Commun. **44**, 1041 (1981); J. C. Gill, in *Charge Density Waves in Solids,* Vol. 217 of *Lecture Notes in Physics,* edited by Gy. Hutiráy and J. Sólyom (Springer-Verlag, Berlin, 1985), p. 377.

[19] T. Chen, L. Mihály, and G. Grüner, Phys. Rev. Lett. **60**, 464 (1988); G. Mihály, T. Chen, and G. Grüner, Phys. Rev. B **38**, 12 740 (1988).

[20] P. Monceau, in the first of Ref. 2, Fig. 27, p. 195.

[21] J. R. Tucker, W. G. Lyons, and G. Gammie, Ref. 6, p. 1164.

[22] K. Maki, Phys. Rev. B **33**, 2852 (1986).

[23] M. Weger, G. Grüner, and W. G. Clark, Solid State Commun. **44**, 1179 (1982).

[24] R. E. Thorne, W. G. Lyons, J. W. Lyding, J. R. Tucker, and J. Bardeen, Phys. Rev. B **35**, 6348 (1987); R. E. Thorne, J. S. Hubacek, W. G. Lyons, J. W. Lyding, and J. R. Tucker, *ibid.* **37**, 10 055 (1988).

[25] J. H. Ross, Jr., Z. Wang, and C. P. Slichter, Phys. Rev. Lett. **56**, 663 (1986).

[26] J. H. Ross, Jr., Ph.D. thesis, University of Illinois at Urbana-Champaign, 1986.

[27] A. Jánossy, C. Bertier, P. Ségransan, and P. Butaud, Phys. Rev. Lett. **59**, 2348 (1987).

[28] T. Csiba, G. Kriza, and A. Jánossy (unpublished).

[29] P. Ségransan, A. Jánossy, C. Berthier, J. Marcus, and P. Butaud, Phys. Rev. Lett. **56**, 1854 (1986).

[30] S. H. Strogatz, C. M. Marcus, R. M. Westervelt, and R. E. Mirollo, Phys. Rev. Lett. **61**, 2380 (1980).

[31] M. Inui, R. P. Hall, S. Doniach, and A. Zettl, Phys. Rev. B **38**, 13 047 (1988).